PRP Pharmacology Research & Perspectives
Open Access

ORIGINAL ARTICLE

In vitro pharmacological profiling of R406 identifies molecular targets underlying the clinical effects of fostamatinib

Michael G. Rolf, Jon O. Curwen, Margaret Veldman-Jones, Cath Eberlein, Jianyan Wang, Alex Harmer, Caroline J. Hellawell & Martin Braddock

AstraZeneca R&D Alderley Park, Macclesfield, Cheshire SK10 4TG, United Kingdom

Keywords
Blood pressure elevation, fostamatinib, in vitro pharmacological profiling, R406, SYK

Correspondence
Michael G. Rolf, AstraZeneca R&D Mölndal, Pepparedsleden 1, 431 83 Mölndal, Sweden. Tel: +46 31 776 60 40; Fax: +46 31 776 37 60; E-mail: mike.rolf@astrazeneca.com

Funding Information
No funding information provided.

Received: 9 April 2015; Accepted: 14 July 2015

Pharma Res Per, 3(5), 2015, e00175, doi: 10.1002/prp2.175

doi: 10.1002/prp2.175

Abstract

Off-target pharmacology may contribute to both adverse and beneficial effects of a new drug. In vitro pharmacological profiling is often applied early in drug discovery; there are fewer reports addressing the relevance of broad profiles to clinical adverse effects. Here, we have characterized the pharmacological profile of the active metabolite of fostamatinib, R406, linking an understanding of drug selectivity to the increase in blood pressure observed in clinical studies. R406 was profiled in a broad range of in vitro assays to generate a comprehensive pharmacological profile and key targets were further investigated using functional and cellular assay systems. A combination of traditional literature searches and text-mining approaches established potential mechanistic links between the profile of R406 and clinical side effects. R406 was selective outside the kinase domain, with only antagonist activity at the adenosine A_3 receptor in the range relevant to clinical effects. R406 was less selective in the kinase domain, having activity at many protein kinases at therapeutically relevant concentrations when tested in multiple in vitro systems. Systematic literature analyses identified KDR as the probable target underlying the blood pressure increase observed in patients. While the in vitro pharmacological profile of R406 suggests a lack of selectivity among kinases, a combination of classical searching and text-mining approaches rationalized the complex profile establishing linkage between off-target pharmacology and clinically observed effects. These results demonstrate the utility of in vitro pharmacological profiling for a compound in late-stage clinical development.

Abbreviations

2-Cl-IB-MECA, (2S,3S,4R,5R)-5-[2-chloro-6[(3-iodophenyl)methylamino]purin-9-yl]-3,4-dihydroxy-N-methyloxolane-2-carboxamide; 2D, two-dimensional; 3D, three-dimensional; CHO, chinese hamster ovary; DAPK1, death-associated protein kinase 1; DMSO, dimethylsulphoxide; FLT3, Fms-like tyrosine kinase 3; GTPγS, guanosine 5′-O-[gamma-thio]triphosphate; HPLC, high-performance liquid chromatography; HUVEC, human umbilical vein endothelial cell; ITP, immune thrombocytopenic purpura; KIT, mast/stem cell growth factor receptor; RA, rheumatoid arthritis; SRC, proto-oncogene tyrosine-protein kinase Src; STK16, serine-threonine protein kinase 16; SYK, spleen tyrosine kinase; TYRO3, tyrosine-protein kinase receptor TYRO3.

Introduction

A new drug is typically developed to target a specific biological molecule in order to treat the symptoms or modulate the underlying causes of a disease. However, very few if any small molecule drugs are truly specific for the intended primary target and unintended off-target interactions may drive adverse drug reactions or, in some cases, contribute to the efficacy of the drug. In vitro pharmacological profiling has been demonstrated to add value in the drug discovery process by influencing chemical design with the objective of selecting a compound with low promiscuity, maximizing the chances of success and minimizing the risk of intolerable side effects (Bowes et al. 2012). Off-target pharmacology may not be restricted to targets closely related to the intended therapeutic target (Paolini et al. 2006), and consideration should be given to the most appropriate technologies and test systems to use (Bowes et al. 2012). Prospectively, the data can be used to differentiate between different chemical series and to predict possible adverse drug reactions (Whitebread et al. 2005; Peters et al. 2012). Retrospectively, the profile can provide mechanistic insight into the effects seen in preclinical and clinical studies. Linking an adverse effect to a molecular target can enable informed decisions to be made about study exclusion criteria to ensure patients' safety, or mitigate the need for broad-based warnings in labeling. Off-target pharmacology can also support additional indications for marketed drugs. For example, the inhibitory activity of quetiapine fumarate and particularly its metabolite *N*-desalkylquetiapine on the noradrenaline transporter that was initially detected via broad in vitro pharmacological profiling provides part of the basis for the efficacy of this compound in depressive disorders (Goldstein et al. 2007; Jensen et al. 2008).

Fostamatinib (previously known as R788) is the first small molecule oral spleen tyrosine kinase (SYK) inhibitor (Braselmann et al. 2006; Riccaboni et al. 2010; Singh et al. 2012), which has completed phase III clinical trials in patients with rheumatoid arthritis (RA; Weinblatt et al. 2013) and is currently in phase 3 trials for immune thrombocytopenia purpura (ITP) (http://www.rigel.com/rigel/pipeline).

Spleen tyrosine kinase is expressed in cells of the hematopoietic lineage such as mast cells, basophils, B-cells, T-cells, neutrophils, dendritic cells, macrophages, monocytes, erythrocytes, and platelets in addition to nonhematopoietic cells such as osteoclasts, vascular endothelial cells, fibroblasts, hepatocytes, and neuronal cells (reviewed in De Castro 2011; Singh et al. 2012). Spleen tyrosine kinase is an intracellular protein kinase and is a key mediator of Fc and B-receptor signaling found on the surface of inflammatory cells where it acts at the head of a signaling cascade and is thought to mediate a diverse set of cellular responses in RA and in the periphery. Spleen tyrosine kinase signaling is an integral component of auto-antibody activation of immune cells (Wong et al. 2004) and inhibition of SYK may, therefore, reduce the autoimmune response (Braselmann et al. 2006). Fostamatinib modulates immune signaling in multiple cell types involved in inflammation and tissue damage in rheumatoid arthritis and so may inhibit key steps in the progression of this disease (Wong et al. 2004). In phase II clinical studies for RA (Weinblatt et al. 2008, 2010), fostamatinib has been associated with an increase in systolic blood pressure of approximately 3 mmHg between baseline at month 1, as compared with a decrease of 2 mmHg with placebo. Preclinical studies suggest that alterations in nitric oxide production in the endothelium may underlie these increases (Skinner et al. 2014). Fostamatinib itself is a prodrug, rapidly metabolized in vivo to the pharmacologically active moiety R406 (Baluom et al. 2013) and therefore in vitro studies investigating the mechanisms underlying the in vivo actions of fostamatinib utilize R406. As a member of the tyrosine kinase class inhibitor class of compounds, R406 like other members of the class exhibits activity at other kinase targets (Metz et al. 2011; Davis et al. 2011), although this is reduced when compared with SYK inhibition in assays of cellular function (Braselmann et al. 2006). In a limited panel of nonkinase targets, R406 had few off-target activities outside of the kinase space (Braselmann et al. 2006), and this study did not identify a molecular target that could link to the increases in blood pressure seen in preclinical and clinical studies. However, this assessment focused on receptors, ion channels, and transporters, thereby omitting a number of target classes known to be commonly hit by kinase inhibitors, for example, phosphodiesterases (Luke et al. 2008). A broader profiling exercise, utilizing multiple technologies, is therefore required. In the current study, we present the most comprehensive in vitro pharmacological profile published to date for a compound in late-stage clinical trials and describe the links between individual targets and the observed effects of fostamatinib in patients.

Materials and Methods

Determination of the solubility of R406

R406 was synthesized by AstraZeneca. The solubility of R406 in 100% DMSO and in eight assay buffers representative of the compositions used in the in vitro assays was determined.

An R406 DMSO solution was diluted with the buffer used in kinase assay until the solubility limit was achieved. The resulting mixture was vortexed well. An ali-

quot was taken at 3 and 24 h, which was centrifuged at 10,000 xg for 10 min at 25°C. The supernatant was mixed with an equal volume of acetonitrile and the suspension was centrifuged again at 10,000 xg for 10 min at 25°C. The resulting supernatant was analyzed by HPLC to determine the solubility.

In vitro pharmacological profiling of R406 in a diverse panel of assays

Radioligand binding assays were used to assess the ability of R406 to interact with receptors, ion channels, and transmembrane transporters; assays measuring substrate turnover by isolated proteins were used for enzyme targets. R406 was tested initially at a single concentration of 10 μmol/L in duplicate, in 322 assays, covering 314 distinct molecular targets and concentration–response curves were generated for targets with ≥50% inhibition in the initial screen. For two targets where the binding K_i of R406 was <1 μmol/L, in vitro functional assays were used to further characterize R406 at these targets. The mode of action of R406 at the adenosine A_3 receptor was investigated using human A_3 receptors expressed in CHO cells, measuring GTPγS binding in the absence and presence of the A_3 agonist 2-Cl-IB-MECA. Functional activity at the adenosine transporter was assessed by measuring uptake of [^{3}H]adenosine into U937 cells. For enzyme targets, substrate turnover assays measuring the activity of isolated, purified enzymes were used; unlike radioligand binding assays, these assays gave a direct determination of the mode of action of R406 so no further follow-up was required. As for the radioligand binding assays, a 10 μmol/L (duplicate) initial screen was used and concentration–response curves generated for targets with ≥50% inhibition in the initial screen. In all assay types, concentration–response curves used eight concentrations in half-log steps, with the IC_{50} value (and K_i where appropriate, Cheng and Prusoff 1973) determined by fitting a four-parameter logistic equation to the data, with the top and bottom of the curve set to 100 and 0, respectively. All assays were performed at Eurofins Panlabs, Ltd., Taiwan, using standard experimental techniques; details of all assays including experimental protocols are described at https://www.eurofinspanlabs.com/catalog/assaycatalog/assaycatalog.aspx.

In vitro profiling of R406 in kinase binding assays

The KINOME*scan*™ binding technology utilized in this study has been described in detail elsewhere (Fabian et al. 2005). Briefly, human kinases were expressed as fusions to T7 bacteriophage and a range of biotinylated small molecule ligands were immobilized on streptavidin-coated magnetic beads. Phage-kinase fusions, ligand affinity beads, and R406 were incubated for 1 h at room temperature. The beads were washed, and the remaining kinase was quantified via qPCR. R406 was tested initially at a single concentration of 10 μmol/L in duplicate, in 387 assays for wild-type kinases. Concentration–response curves were generated for a total of 260 assays. One hundred and ninety-two assays were tested in singlicate only; a subset of 68 kinases was tested in duplicate or triplicate to investigate the overlap and differences between published datasets and between the binding technology and radiometric enzyme activity assays.

In vitro profiling of R406 in functional kinase assays

In vitro functional assays were performed at Millipore, UK, using the technique described by Gao et al. (2013). Purified human recombinant kinases were expressed either as full length proteins or catalytically active fragments, and incubated in assay buffers with peptide or protein substrate, γ-^{33}P-ATP and R406. After incubation, the reactions were stopped with 3% phosphoric acid, reaction medium spotted onto filter paper, washed, and radioactivity quantified via scintillation counting. Full details of assay conditions are available at http://www.millipore.com/techpublications/tech1/pf3036. Concentration–response curves were constructed in triplicate, with nine half-log steps from 1 nmol/L up to 10 μmol/L.

Text mining of literature to identify kinases associated with blood pressure changes in humans

One hundred kinases were selected for detailed analysis, based on having an IC_{50} value <150 nmol/L in one or both of the in vitro binding and functional assays. A search of Medline abstracts was performed, seeking sentence-level co-occurrence of any of the 100 kinase names of interest (and synonyms) with a list of terms related to blood pressure. Since the focus of our studies was directed against understanding and interpreting clinical trial data, the search strategy included a restriction to papers relevant to humans only. Data were manually curated to remove ambiguous hits that had detected unrelated terms or abbreviations matching the kinase search terms.

Investigation of the effects of R406 on VEGF-stimulated endothelial cell development in vitro

The effect of R406, in a concentration range from 3 nmol/L to 1 μmol/L, on VEGF-dependent signaling was

investigated in two in vitro human fibroblast–endothelial cell coculture assay systems where cell growth is driven by VEGF stimulation, as described by Kendrew et al. (2011). In the two-dimensional (2D) system, R406 was incubated for 11 days in the presence of 3 ng/mL VEGF-A, and tube formation was visualized by staining HUVEC cells with a CD31 antibody. Tube length measured in mm was quantified by image analysis. The three-dimensional (3D) system utilized beads coated in endothelial cells and fibroblasts were suspended in Matrigel in the presence of 5 ng/mL VEGF-A. R406 was incubated at a range of concentrations for 7 days, and tube formation was visualized by staining HUVEC cells with a CD31-Alexa-tagged antibody.

Translation of in vitro KDR inhibition to blood pressure increases in humans

To assess the translation of KDR (VEGFR2) inhibition to increased blood pressure in clinical trials, we compared the in vitro potency of five reference kinase inhibitors and R406 at KDR, as measured in HUVEC cells, with the degree of blood pressure elevation reported for each compound from clinical trials. KDR IC_{50} and plasma concentration data were taken from the report of McTigue et al. (2012). Data on blood pressure changes were sourced from the literature (Veronese et al. 2006; Robinson et al. 2010; Weinblatt et al. 2010; Genovese et al. 2011; Mayer et al. 2011; Eechoute et al. 2012; Heath et al. 2013).

Data analysis and statistical procedures

For kinase binding and activity assays, where multiple replicates were generated (and in the case of kinase binding assays, the multiple replicates could not be reasonably aggregated, for example, where one or more curves did not have a defined midpoint), a global curve fitting approach was used to generate a single estimate of the curve midpoint value for each assay, together with the uncertainty around this value. One curve was fitted to each set of duplicate or triplicate results, with a common midpoint value. The nonlinear regression fitting the sigmoidal dose–response curves was performed using GraphPad Prism version 4.03 for Windows, GraphPad Software, San Diego, CA, www.graphpad.com.

Results generated in different kinase assay technologies were compared by plotting the difference in IC_{50} values determined in the two technologies to the mean IC_{50} value across both technologies, to identify systematic bias or dependency on potency (Altman and Bland 1983).

Results

R406 has variable solubility in DMSO and in vitro assay buffer systems

R406 was soluble in DMSO up to ~140 mmol/L. Solubility in phosphate-buffered saline at physiological pH was very low (0.2 μmol/L) and pH dependent, with solubility increasing markedly at acidic pH (<3). In some cases, increasing the DMSO content over the range 0.1–1% slightly increased solubility but the improvements were limited. The presence of either a surfactant such as Tween-20, Triton X-100, or Brij-35, or bovine serum albumin greatly increased solubility from <1 μmol/L to 10 μmol/L or more. Full results are presented in Table S1.

R406 is selective when profiled across multiple target classes

In the broad in vitro panel covering 314 diverse molecular targets, when tested at 10 μmol/L R406 showed >50% inhibition at nine targets. Concentration–response curves were generated and IC_{50} and K_i (where applicable) values were calculated (Table 1). The full profile is provided in Table S2. For targets with K_i values <1 μmol/L, in vitro functional assays were used to characterize the mode of action of R406 (Table 1). For the adenosine A_3 receptor, R406 on its own at concentrations up to 10 μmol/L had

Table 1. Quantification of nonkinase off-target activities of R406.

Target	Radioligand binding or enzyme activity IC_{50} (nmol/L)	Radioligand binding K_i (nmol/L)	Mode of action
Adenosine A_3 receptor (human)	18	17	Antagonist
UDP glucuronosyltransferase UGT1A1 (human)	143	NA[1]	Inhibitor
Phosphodiesterase PDE5 (human)	308	NA	Inhibitor
Adenosine transporter (human)	1860	634	Inhibitor
Fatty acid amide hydrolase (rat)	1510	NA	Inhibitor
Vesicular monoamine transporter (rabbit)	1960	1630	ND[2]
5-Lipoxygenase (human)	5500	NA	Inhibitor
Cathepsin L (human)	5930	NA	Inhibitor
Cathepsin S (human)	11,900	NA	Inhibitor

[1]Not applicable.
[2]Not determined.

no effect. R406 reduced the GTPγS binding stimulated by the specific A_3 agonist 2-Cl-IB-MECA, with an IC_{50} value of 410 nmol/L. These results are consistent with antagonist activity at the human adenosine A_3 receptor, taking into account the expected shift in potency in the presence of an agonist (compared to the "ligand-free" affinity measure from the radioligand binding assay). An assay measuring the uptake of [^{3}H]adenosine into U937 cells was used to further investigate the ability of R406 to prevent adenosine uptake. In this assay system, which expresses both equilibrative and concentrative nucleoside transporters, R406 inhibited adenosine uptake with an IC_{50} of 100 nmol/L (compared to the binding affinity of 634 nmol/L), confirming that R406 can act as a functional inhibitor of adenosine uptake.

R406 binds to multiple kinases at therapeutically relevant concentrations

R406 was profiled in a total of 387 in vitro binding assays for individual kinases, to build the broadest possible kinase activity profile for the compound. In the initial 10 μmol/L single concentration screen, R406 inhibited the qPCR signal by 80% or more for 197 kinases. Two hundred and sixty kinases were selected for further experiments to characterize concentration–response curves including the 197 which showed ≥80% inhibition, plus a further 63 of the profiled kinases that were reported to be targets for R406 in an earlier study (Davis et al. 2011). Calculated K_d values ranged from 0.5 nmol/L (STK16) up to 11.58 μmol/L (TYRO3); concentration–response curves could not be satisfactorily fitted for 22 kinases primarily due to incomplete curves with incompletely defined maxima. K_d values are summarized in Figure 1; full results in tabular form are included in Table S3.

R406 inhibits multiple kinases in in vitro functional assays

Based on the results from the kinase binding experiments, together with existing data from a range of in vitro kinase activity assays (data not shown), 139 kinases were selected for further screening in in vitro isolated kinase activity assays. Concentration–response curves were generated in triplicate, and a single IC_{50} value for each kinase derived using a global fit methodology. One hundred and twenty IC_{50} values were calculated, ranging from 3 nmol/L (FLT3) to 3.49 μmol/L (DAPK1), with R406 inactive in the remaining 19 kinases (median estimate of curve top showing <50% inhibition). Kinase activity data are summarized in Figure 2 and the full is dataset included in Table S3.

Different kinase assay technologies produce different activity profiles

For the 136 kinases with both binding and enzyme activity data, R406 was active (having a defined IC_{50} or K_d value) in 117 assays, and inactive in the activity assay for the remaining 19 kinases. The inverse (active in

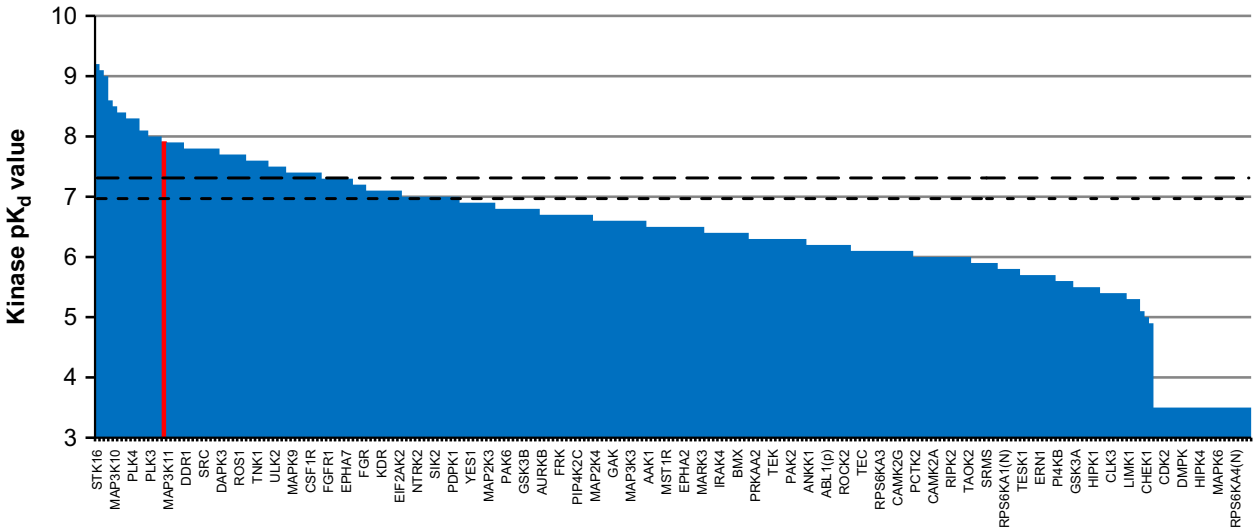

Figure 1. R406 binds to a wide range of protein kinase targets. Kinase binding pK_d values for 260 kinases are represented by the blue bars; for clarity, spleen tyrosine kinase is highlighted in red (not all kinases are identified on the *x*-axis). Dashed black lines indicate the maximum free plasma concentrations achieved in TASKI-2 (long dashes) and the thorough QT study (short dashes). Kinases where a pK_d value could not be determined have been assigned a value of 3.5 for the purpose of inclusion on the plot.

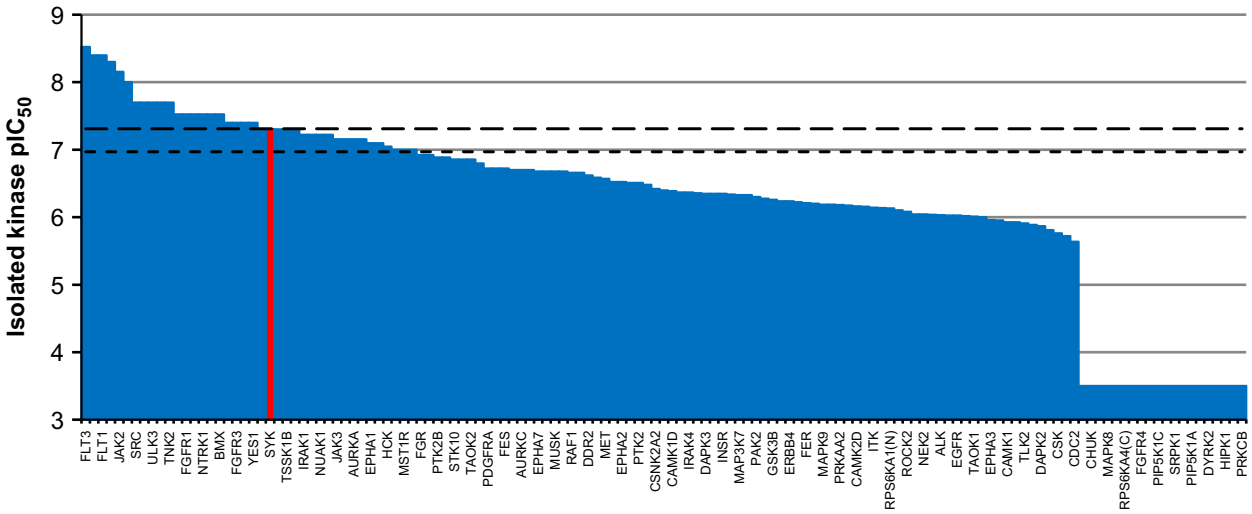

Figure 2. R406 functionally inhibits a range of isolated kinases in vitro. Isolated enzyme kinase activity assay pIC_{50} values for 139 kinases tested at or near the K_m for ATP are represented by the blue bars. For clarity, spleen tyrosine kinase is highlighted in red (not all kinases are identified on the *x*-axis). Dashed black lines indicate the maximum free plasma concentrations achieved in TASKI-2 (long dashes) and the thorough QT study (supratherapeutic 300 mg bid dose, short dashes). Kinases where a pIC_{50} value could not be determined have been assigned a value of 3.5 for the purpose of inclusion on the plot.

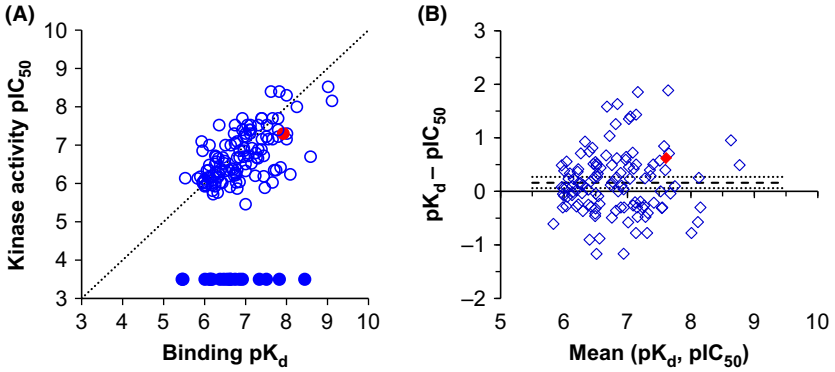

Figure 3. Comparison of the kinase profile of R406 in different assay technologies. (A) pIC_{50} from the radiometric substrate turnover assays plotted against pK_d from the displacement binding assays; 136 kinases are represented on the plot. Spleen tyrosine kinase is highlighted in red. The black line indicates the line of equivalence. Kinases where R406 was inactive in the substrate turnover assay were assigned a pIC_{50} value of 3.5, for the purposes of inclusion on the plot. (B) Altman–Bland plot comparing the two technologies. The dashed line indicates the mean difference between the technologies (0.16 log units), with the dotted lines being the 95% upper and lower confidence limits of this difference.

enzyme activity, inactive in binding) could not be assessed using the experimental design described here since the enzyme activity assays were selected based on R406 showing activity in the corresponding binding assays. There was little or no correlation between the two technologies (Fig. 3A), even if the 19 inactive kinase activity assays were excluded ($r^2 = 0.38$ in this case). A comparison of the two technologies using methodology previously described (Altman and Bland 1983; Fig. 3B), indicated that there was no evidence for dependence on the mean of the K_d and IC_{50} values, but there was a bias between the methods, with the kinase activity technology on average giving slightly lower potency values (by ~0.2 log unit).

Identification of kinases associated with changes in blood pressure in humans

In order to identify key kinase(s) for further experimental evaluation, the list of kinases where R406 had a quantified activity (binding K_d or functional IC_{50}) within threefold of the SYK functional IC_{50} of 50 nmol/L was examined for association to blood pressure changes. The list compromised 100 kinases. Text mining of the PubMed

database (current at 30/03/2013) for links between individual kinases and hypertension identified a total of 157 papers, with sentence-level co-occurrence of kinase and blood pressure terms for 27 kinases; no literature evidence for a relationship with blood pressure was found for the remaining 73 kinases. The therapeutic target SYK was linked to a single paper (Weinblatt et al. 2010). Among the remaining 26 kinases linked to blood pressure, only four kinases were specifically recognized in five or more papers: FLT1 (83 papers), KDR (16 papers), SRC (five papers), and KIT (five papers).

R406 inhibits VEGF-mediated signaling in intact cells

Based on the literature evidence for a connection to hypertension, the ability of R406 to inhibit VEGF-A-dependent signaling using 2D and 3D in vitro human fibroblast–endothelial coculture cell assays was investigated. R406 inhibited human endothelial cell tube formation and tube outgrowth driven by exogenous VEGF with EC_{50} values of 47.3 ±11 nmol/L (2D tube formation) and 21.4 ±3.4 nmol/L (3D HUVEC outgrowth assay). Representative images are presented in Figure 4.

Translation of in vitro KDR inhibition to hypertension in clinical trials

Figure 5A shows the magnitude of hypertension observed in clinical trials for a range of KDR inhibitors with in vitro potencies in the range 0.088–333 nmol/L. There is no clear correlation between the in vitro potency and the degree of hypertension. For example, cediranib is ~31-fold more potent at KDR than sunitinib, yet causes a smaller mean increase in systolic blood pressure; sorafenib and vandetanib cause similar increases in diastolic blood pressure but the latter is ~26-fold less potent at KDR. This analysis does not take into account the therapeutic plasma concentration of each kinase inhibitor, and to address this limitation, we divided the in vitro IC_{50} for KDR inhibition in a HUVEC assay system by the maximum free plasma concentration of drug in clinical trials to generate a ratio where values >1 indicate that the free exposure equals a level greater than the in vitro IC_{50} value. The degree of hypertension observed in clinical trials was then plotted against this value (Fig. 5B) to give a more relevant assessment of the effect of KDR inhibition on blood pressure.

Discussion and Conclusions

Drugs often have off-target activities outside the class of the intended therapeutic target (Paolini et al. 2006) and in vitro pharmacological profiling is widely used to characterize the selectivity of candidate compounds (Bowes et al. 2012). A broad pharmacological profile covering a range of target classes will utilize multiple in vitro technologies. When interpreting in vitro data it is important to consider both the characteristics of the test compound and the assay systems used. R406 is highly soluble in DMSO but dilution into aqueous protein-free media leads to a considerable drop in solubility, limiting the test concentrations and making it difficult to fully characterize concentration–response relationships covering a range relevant to the therapeutic free plasma concentration. This study reinforces the robustness of the selectivity profile reported by Braselmann et al. (2006) and extends it to cover a much broader range of target classes including, for example, enzymes other than kinases.

Even within a technology, methodology differences may confound interpretation. In the kinase binding assays used in this study, different dilution protocols are used for single concentration (10 μmol/L) and concentration–response tests. This may explain the minor differences between the kinase profiles reported here and by Davis et al. (2011); of 27 kinases differentially classified as active or inactive between the two studies, all but one have reported K_d values >1 μmol/L (the range when R406 solubility limits the accuracy of K_d determination and also the threshold for false-negative detection in this assay system, Fabian et al. 2005). Comparison of the activity datasets presented here and by Metz et al. (2011) reveals a similar pattern (data not shown).

In the present study, the use of two distinct technologies to measure kinase activities highlights some of the challenges in conclusively defining the profile of a kinase inhibitor. The inhibitor displacement technology provides broad kinome coverage with a single technology, and independence from ATP concentration. However, it does not provide a direct measure of enzyme activity inhibition and inferences must be drawn between compound binding and potential functional inhibition. Radiometric substrate turnover assays address this latter limitation, but introduce potential variability due to the concentration of ATP in the assay system (here set at or near to K_m to optimize sensitivity but not necessarily reflecting the concentration in intact cells). We found that while the two technologies gave qualitatively similar results (i.e., R406 was active in both technologies, at any given kinase, in most cases), there was not a quantitative correlation between the technologies. Therefore, for further interpretation we combined the results of both technologies, classifying any kinase where R406 was active in either technology as active in the overall profile.

Having established an in vitro pharmacological profile for R406, we addressed the relevance to effects observed in

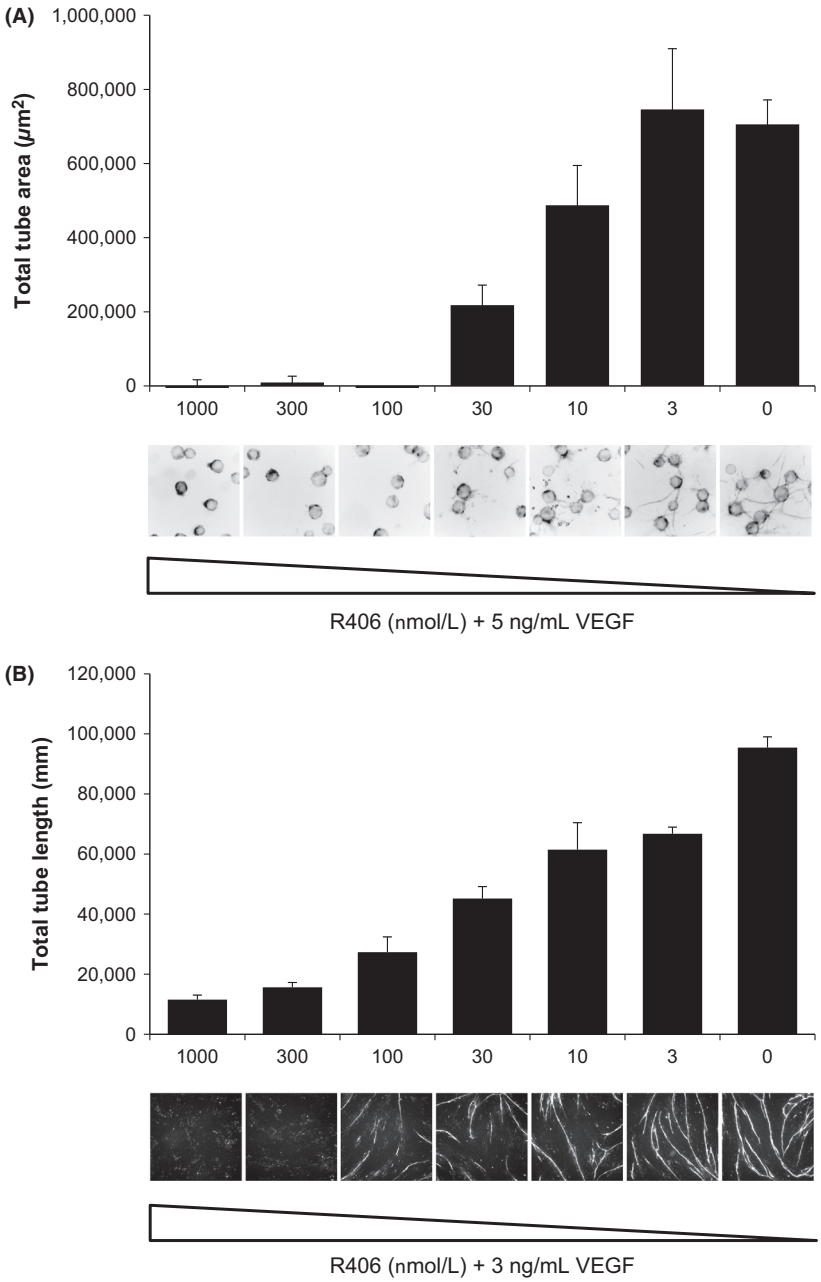

Figure 4. R406 inhibits endothelial tube formation. (A) R406 was tested for its ability to inhibit endothelial tube formation in a fibroblast–endothelial 2D coculture system. R406 was incubated at a range of concentrations for 11 days, and tube formation was visualized by staining HUVEC cells with a CD31 antibody. Tube length measured in mm was quantified by image analysis. Representative images captured at ×25 magnification are shown. Data are representative of more than three identical experiments. (B) R406 was tested for the ability to reduce tubule formation in a 3D outgrowth assay. Beads coated in endothelial cells and fibroblasts were suspended in Matrigel in the presence of 5 ng/mL VEGF-A. R406 was incubated at a range of concentrations for 7 days, and tube formation was visualized by staining HUVEC cells with a CD31-Alexa-tagged antibody. Representative images captured at ×25 magnification are shown. Data are representative of more than three identical experiments.

patients treated with fostamatinib. In phase II clinical studies for RA (Weinblatt et al. 2008, 2010), fostamatinib has been associated with an increase in systolic blood pressure of approximately 3 mmHg between baseline at month 1, as compared with a decrease of 2 mmHg with placebo. The free plasma concentration of a drug drives pharmacological effects (Smith et al. 2010) and so the peak free exposures achieved in clinical trials can be used as a threshold to define the interesting portion of the in vitro profile. Across a range of drugs (primarily targeting G-protein coupled

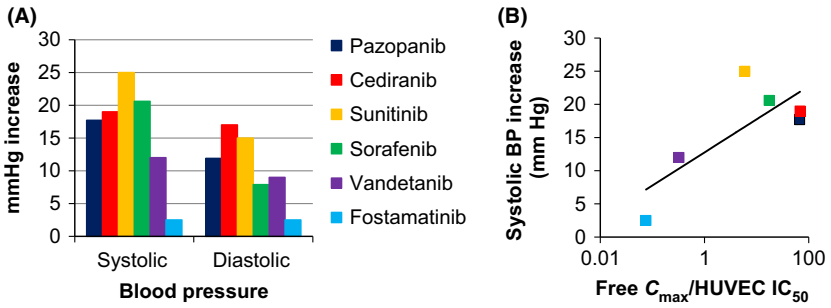

Figure 5. Degree of KDR inhibition in vitro at therapeutically relevant concentrations predicts increase in blood pressure in the clinic. (A) Mean increases in systolic and diastolic pressures recorded during clinical trials, for six KDR inhibitors including fostamatinib. (B) Mean systolic blood pressure increase plotted against the KDR IC_{50} (in HUVEC cells) divided by the clinical maximum free plasma concentration. A value >1 for this ratio indicates that the maximum free plasma exposure exceeds the IC_{50} in the HUVEC cell assay. The black line indicates the linear correlation, $r^2 = 0.61$. Color coding as identified in the legend for Figure 5A.

receptors) and indications it has been shown that a free plasma concentration of 1–3 times the in vitro affinity at the intended target is required to drive the therapeutic effect (McGinnity et al. 2007; Smith et al. 2010). In RA patients receiving fostamatinib (100 mg bid) C_{max} values were 762 ± 234 ng/mL, which is equivalent to an unbound R406 concentration of 28 nmol/L (Baluom et al. 2011). This peak free plasma concentrations is ~2.5-fold higher than the in vitro displacement binding K_d value for SYK determined in this study (12 nmol/L) and comparable to the isolated enzyme activity IC_{50} value (50 nmol/L). Fostamatinib therefore appears to fit into the same relationship for its therapeutic target. Making the assumption that a similar relationship could exist for off-target effects, and adding a threefold margin to account for the variability inherent in biological systems, we selected a threshold potency of 150 nmol/L above which any target is considered unlikely to be contributing significantly to effects observed in patients.

Applying this cut-off to the profile of R406 identifies 101 targets of interest, of which the adenosine A_3 receptor is the only nonkinase. R406 is an antagonist at this receptor, and there is no evidence in the literature for A_3 antagonists increasing blood pressure in animal models. The expression and pharmacology of A_3 receptors differ significantly between rodents and humans (Ijzerman et al. 2013), so animal models may not adequately represent human pharmacology. However, no selective A_3 antagonists have been tested in man to date. In phase II clinical trials for RA with the A_3 agonist CF101, the main adverse effects reported were mild headache, nausea, and rash with no adverse effects on blood pressure (Silverman et al. 2008). Recently, the selective A_3 antagonist SSR161421 has been reported to have beneficial effects in animal models of asthma (Mikus et al. 2013) suggesting that this off-target activity for fostamatinib may confer a potential advantage in some inflammatory diseases.

Deconvolution of the potential biological activity of a profile of at 100 kinases is much more challenging. Practical considerations exclude the possibility of running cell-based assays for every kinase hit as would be considered the norm when investigating activity at the intended therapeutic target. Testing in kinase activity assays with cellular concentrations of ATP (rather than the near-K_m concentrations used in this study) would be an alternative to estimate the potency shift due to competition with ATP in vivo. Again, this approach is suited to a narrow kinase profile only. Instead, we assumed that any of the 100 kinases meeting our 150 nmol/L threshold are possible targets, and applied a literature mining approach to identify those with a robust scientific linkage to blood pressure modulation. The therapeutic target SYK was linked to a single paper, reporting the outcome of a 6 month phase II trial for fostamatinib (Weinblatt et al. 2010). This probably reflects the scarcity of selective SYK inhibitors in late-stage clinical development (and therefore the lack of literature reporting clinical effects in humans – a key filter in our search strategy) and may change in the next few years. Among the remaining 26 kinases linked to blood pressure, five kinases were specifically recognized in five or more papers: FLT1 (83 papers), KDR (16), SRC (5), and KIT (5). More detailed examination of the papers linked to SRC revealed that activation of SRC may lead to hypertension; inhibition of SRC has been shown to cause hypotension in preclinical species but not in humans (unpubl. obs.). The level of KIT in peripheral blood is an independent predictor of both systolic and diastolic blood pressure (Zhong et al. 2010) and the kinase has been proposed as a therapeutic target for idiopathic pulmonary arterial hypertension (Montani et al. 2011). Imatinib inhibits Bcr-Abl, KIT, and PDGF receptors, and in multiple clinical trials is not associated with hypertension (Van Oosterom et al. 2001; Demetri et al. 2002). Other drugs targeting KIT that cause hyper-

tension are also potent inhibitors of VEGF receptor kinases, activity that is not shared by imatinib.

The remaining two kinases, FLT1 and KDR, are VEGF receptors. Drug-induced blood pressure elevation is a recognized effect of receptor tyrosine kinase inhibitors whose pharmacological profile includes blockade of VEGF receptors (Pullamsetti and Schermuly 2009). Inhibitors of the VEGF pathway can modulate blood pressure and induce hypertension in patients (Eskens and Verweij 2006; Sica 2006; Van den Meiracker et al. 2012), an effect primarily mediated through KDR (Li et al. 2002). The incidence and magnitude of hypertension observed in clinical trials correlate to the drugs' activities against KDR (Bhargava 2009; and this study). As demonstrated here, R406 inhibits VEGF receptor tyrosine kinases in all assay formats tested (isolated kinases and cell-based models) and across species (Lengel D, Lamm Bergström E, Barthlow H, Oldman K, Musgrove H, Harmer A, Valentin J-P, Duffy P, Braddock M & Curwen J, in press). Recent work by Skinner et al. (2014) extends this characterization into in vivo systems, confirming the effects of R406 on vascular endothelium and blood pressure in preclinical models. Hypertension caused by VEGF receptor tyrosine kinase inhibitors has been successfully managed using traditional antihypertensive regimes (Langenberg et al. 2009), and based on the evidence presented here for a similar mechanism, these regimes have been shown to be effective in nonclinical models (Lengel D, Lamm Bergström E, Barthlow H, Oldman K, Musgrove H, Harmer A, Valentin J-P, Duffy P, Braddock M & Curwen J, in press). We would therefore expect that these regimes would be effective in managing blood pressure increases in patients receiving fostamatinib.

In summary, in this study we have utilized broad in vitro pharmacological profiling to characterize R406 and demonstrated how the knowledge of the drug's off-target pharmacology can be interpreted and used to develop credible and testable mechanistic hypotheses explaining clinical effects observed in patients. This understanding can be used to underpin risk mitigation and management strategies with a scientific rationale.

Acknowledgements

The authors thank Marie South for statistical advice and expertise, and J. Bowes for comments on the manuscript.

Author Contributions

M. G. R., J. O. C., M. V.-J., C. E., J. W., and A. H. designed the experiments. M. V.-J. and C. E. performed tube formation assays and J. W. performed the solubility assays. C. J. H. performed text-mining analyses. All authors contributed to the final manuscript.

Disclosure

All authors are employed by AstraZeneca.

References

Altman DG, Bland JM (1983). Measurement in medicine: the analysis of method comparison studies. The Statistician 32: 307–317.

Baluom M, Samara E, Grossbard EB, Lau DT (2011). Fostamatinib, a SYK-kinase inhibitor, does not affect methotrexate pharmacokinetics in patients with rheumatoid arthritis. J Clin Pharmacol 51: 1310–1318.

Baluom M, Grossbard EB, Mant T, Lau DT (2013). Pharmacokinetics of fostamatinib, a spleen tyrosine kinase (SYK) inhibitor, in healthy human subjects following single and multiple oral dosing in three phase I studies. Br J Clin Pharmacol 76: 78–88.

Bhargava P (2009). VEGF kinase inhibitors: how do they cause hypertension? Am J Physiol Integr Comp Physiol 297: R1–R5.

Bowes J, Brown AJ, Hamon J, Jarolimek W, Sridhar A, Waldron G, et al. (2012). Reducing safety-related drug attrition: the use of in vitro pharmacological profiling. Nat Rev Drug Disc 11: 909–922.

Braselmann S, Taylor V, Zhao H, Wang S, Sylvain C, Baluom M, et al. (2006). R406, an orally available spleen tyrosine kinase inhibitor blocks Fc receptor signaling and reduces immune complex-mediated inflammation. J Pharm Exp Ther 319: 998–1008.

Cheng Y-C, Prusoff WH (1973). Relationship between the inhibition constant (K_i) and the concentration of inhibitor which causes 50 per cent inhibition (I_{50}) of an enzymatic reaction. Biochem Pharmacol 22: 3099–3108.

Davis MI, Hunt JP, Herrgard S, Ciceri P, Wodicka LM, Pallares G, et al. (2011). Comprehensive analysis of kinase inhibitor selectivity. Nat Biotech 29: 127–132.

De Castro R (2011). Regulation and function of SYK tyrosine kinase in mast cell signaling and beyond. J Signal Transduct 2011: 507291. doi:10.1155/2011/507291.

Demetri GD, von Mehren M, Blanke CD, van den Abbeele AD, Eisenberg B, Roberts PJ, et al. (2002). Efficacy and safety of imatinib mesylate in advanced gastrointestinal stromal tumours. New Engl J Med 347: 472–480.

Eechoute K, van der Veldt AAM, Oosting S, Kappers MHW, Wessels JAM, Gelderblom H, et al. (2012). Polymorphisms in endothelial nitric oxide synthase (*eNOS*) and vascular endothelial growth factor (*VEGF*) predict sunitinib-induced hypertension. Clin Pharmacol Ther 92: 503–510.

Eskens FA, Verweij J (2006). The clinical toxicity profile of vascular endothelial growth factor (VEGF) and vascular endothelial growth factor receptor (VEGFR) targeting angiogenesis inhibitors: a review. Eur J Cancer 42: 3127–3139.

Fabian MA, Biggs WH, Treiber DK, Atteridge CE, Azimioara MD, Benedetti MG, et al. (2005). A small molecule-kinase interaction map for clinical kinase inhibitors. Nat Biotech 23: 329–336.

Gao Y, Davies SP, Augustin M, Woodward A, Patel UA, Kovelman R, et al. (2013). A broad activity screen in support of a chemogenomic map for kinase signalling research and drug discovery. Biochem J 451: 313–328.

Genovese MC, Kavanaugh A, Weinblatt ME, Peterfy C, DiCarlo J, White ML, et al. (2011). A three-month randomized, placebo-controlled, phase II study in patients with active rheumatoid arthritis that did not respond to biologic agents. Arthritis Rheum 63: 337–345.

Goldstein JM, Christoph G, Grimm S, Liu J, Widzowski D, Brecher M (2007). Quetiapine's antidepressant properties: direct and indirect pharmacologic actions on norepinephrine and serotonin receptors. Eur Neuropsychopharmacol 17(Suppl 4): S401.

Heath EI, Infante J, Lewis LD, Luu T, Stephenson J, Tan AR, et al. (2013). A randomized, double-blind, placebo-controlled study to evaluate the effect of repeated oral doses of pazopanib on cardiac conduction in patients with solid tumours. Cancer Chemother Pharmacol 71: 565–573.

Ijzerman A, Fredholm BB, Jacobson KA, Linden J, Müeller CE (2013). Adenosine receptors: A_3 receptor. Last modified on 09/01/2013. IUPHAR database (IUPHAR-DB), Available at http://www.iuphar-db.org/DATABASE/ObjectDisplayForward?objectId=21 (Accessed on 04 06 2013).

Jensen NH, Rodriguiz RM, Caron MG, Wetsel WC, Rothman RB, Roth BL (2008). *N*-Desalkylquetiapine, a potent norepinephrine reuptake inhibitor and partial 5-HT_{1A} agonist, as a putative mediator of quetiapine's antidepressant activity. J Neuropsychopharmacol 33: 2303–2312.

Kendrew J, Eberlein C, Hedberg B, McDaid K, Smith NR, Weir HM, et al. (2011). An antibody targeted to VEGFR-2 Ig domains 4-7 inhibits VEGFR-2 activation and VEGFR-2-dependent angiogenesis without affecting ligand binding. Mol Cancer Ther 10: 770–783.

Langenberg MHG, van Herpen CML, De Bono J, Schellens JHM, Unger C, Hoekman K, et al. (2009). Effective strategies for management of hypertension after vascular endothelial growth factor signaling inhibition therapy: results from a phase II randomized, factorial, double-blind study of Cediranib in patients with advanced solid tumors. J Clin Oncol 27: 6152–6159.

Li B, Ogasawara AK, Yang R, Wei W, He G-W, Zioncheck TF, et al. (2002). KDR (VEGF receptor 2) is the major mediator for the hypotensive effect of VEGF. Hypertension 39: 1095–1100.

Luke R, Rolf M, Bowes J, Valentin JP (2008). In vitro pharmacological profiles of kinase inhibitors: comparison with other pharmaceuticals. Fund Clin Pharmacol 22(Suppl 2): 59.

Mayer EL, Dallabrida SM, Rupnick MA, Redline WM, Hannagan K, Ismail NS, et al. (2011). Contrary effects of the receptor tyrosine kinase inhibitor vandetanib on constitutive and flow-stimulated nitric oxide elaboration in humans. Hypertension 58: 85–92.

McGinnity DF, Collington J, Austin RP, Riley RJ (2007). Evaluation of human pharmacokinetics, therapeutic dose and exposure predictions using marketed oral drugs. Curr Drug Metab 8: 463–479.

McTigue M, Murray BW, Chen JH, Deng Y-L, Solowiej J, Kania RS (2012). Molecular conformations, interactions, and properties associated with drug efficiency and clinical performance among VEGFR TK inhibitors. Proc Natl Acad Sci USA 109: 18281–18289.

Metz JT, Johnson EF, Soni NB, Merta PJ, Kifle L, Hajduk PJ (2011). Navigating the kinome. Nat Chem Biol 7: 200–202.

Mikus EG, Szeredi J, Boer K, Tímarí G, Finet M, Aranyi P, et al. (2013). Evaluation of SSR161421, a novel orally active adenosine A_3 receptor antagonist on pharmacology models. Eur J Pharmacol 699: 172–179.

Montani D, Perros F, Gambaryan N, Girerd B, Dorfmuller P, Price LC, et al. (2011). C-Kit-positive cells accumulate in remodeled vessels of idiopathic pulmonary arterial hypertension. Am J Resp Crit Care Med 184: 116–123.

Paolini GV, Shapland RHB, van Hoorn WP, Mason JS, Hopkins AL (2006). Global mapping of pharmacological space. Nat Biotech 24: 805–815.

Peters J-U, Hert J, Bissantz C, Hillebrecht A, Gerebtzoff G, Bendels S, et al. (2012). Can we discover pharmacological promiscuity early in the drug discovery process? Drug Disc Today 17: 325–335.

Pullamsetti SS, Schermuly RT (2009). Receptor tyrosine kinases in pulmonary hypertension. PVRI Rev 1: 124–128.

Riccaboni M, Bianchi I, Petrillo P (2010). Spleen tyrosine kinases: biology, therapeutic targets and drugs. Drug Disc Today 15: 517–530.

Robinson ES, Khankin EV, Karumanchi SA, Humphreys BD (2010). Hypertension induced by vascular endothelial growth factor signaling pathway inhibition: mechanisms and potential uses as a biomarker. Semin Nephrol 30: 591–601.

Sica DA (2006). Angiogenesis inhibitors and hypertension: an emerging issue. J Clin Oncol 24: 1329–1331.

Silverman MH, Strand V, Markovits D, Nahir M, Reitblat T, Molad Y, et al. (2008). Clinical evidence for utilization of the

A_3 adenosine receptor as a target to treat rheumatoid arthritis: data from a phase III clinical trial. J Rheumatol 35: 41–48.

Singh R, Masuda ES, Payan DG (2012). Discovery and development of spleen tyrosine kinase (SYK) inhibitors. J Med Chem 55: 3614–3643.

Skinner M, Philp K, Lengel D, Coverley L, Lamm Bergström E, Glaves P, et al. (2014). The contribution of VEGF signalling to fostamatinib-induced blood pressure elevation. Br J Pharmacol 171: 2308–2320.

Smith DA, Di L, Kerns EH (2010). The effect of plasma protein binding on in vivo efficacy: misconceptions in drug discovery. Nat Rev Drug Disc 9: 929–939.

Van den Meiracker AH, Lankhorst S, van Esch JHM, Jan Danser AH, Kappers MHW (2012). Hypertension induced by antiangiogenic therapy: clinical and pathophysiological aspects. Eur J Hosp Pharm 19: 327–329.

Van Oosterom AT, Judson I, Verweij J, Stroobants S, Donato di Paola E, Dimitrijevic S, et al. (2001). Safety and efficacy of imatinib (STI571) in metastatic gastrointestinal stromal tumours: a phase I study. Lancet 358: 1421–1423.

Veronese ML, Mosenkis A, Flaherty KT, Gallagher M, Stevenson JP, Townsend RR, et al. (2006). Mechanisms of hypertension associated with BAY 43-9006. J Clin Oncol 24: 1363–1369.

Weinblatt ME, Kavanagh A, Burgo-Vargas R, Dikranian AH, Medrano-Ramirez G, Morales-Torres JL, et al. (2008). Treatment of rheumatoid arthritis patients with a SYK kinase inhibitor: a twelve week, randomized, placebo-controlled trial. Arthritis Rheum 58: 3309–3318.

Weinblatt ME, Kavanagh A, Genovese MC, Musser TK, Grossbard EB, Magilavy DB (2010). An oral spleen tyrosine kinase (SYK) inhibitor for rheumatoid arthritis. N Engl J Med 363: 1303–1312.

Weinblatt ME, Genovese MC, Ho M, Hollis S, Rosiak-Jedrychowicz K, Kavanaugh A, et al. (2013). Oskira-1: a phase III, multicenter, randomized, double-blind, placebo-controlled parallel-group study of 2 dosing regimens of fostamatinib in rheumatoid arthritis patients with an inadequate response to methotrexate. Arthritis Rheum 65(10 Suppl): S763–S764.

Whitebread S, Hamon J, Bojanic D, Urban L (2005). In vitro safety pharmacology profiling: an essential tool for successful drug development. Drug Disc Today 10: 1421–1433.

Wong BR, Grossbard EB, Payan DG, Masuda ES (2004). Targeting SYK as a treatment for allergic and autoimmune disorders. Exp Opin Invest Drugs 13: 743–762.

Zhong H-L, Lu X-Z, Chen X-M, Yang X-H, Zhang H-F, Zhou L, et al. (2010). Relationship between stem cell factor/c-kit expression in peripheral blood and blood pressure. J Hum Hypertens 24: 220–225.

Supporting Information

Additional Supporting Information may be found in the online version of this article:

Table S1. R406 solubility in a range of buffers.
Table S2. Full in vitro pharmacological profile of R406.
Table S3. Full in vitro kinase profile of R406.